Numerical One-dimensional Advection Equation

Yihang Chen

December 7, 2019

Abstract

In the report, I implement the upwind scheme, Lax-Friedrichs scheme, Lax-Wendroff scheme, and Beam-Warming scheme for the one linear dimensional advection equation. Furthermore, some modifications are adopted to solve the one dimensional quasilinear equation. We implement the upwind type schemes, i.e. the upwind scheme, Roe scheme, Huang scheme and Engquist & Osher scheme, and the second order schemes, i.e. the two-step Richtmyer scheme, Lax-Wendroff scheme and MacCormack scheme. On the quasilinear case, we focus on solving the Burgers' equation. We focus on three types of boundary condition: periodic, infinite and finite Dirichlet boundary condition. Numerical results are included in the report, codes and figures are affiliated in the folder, since the convergence rate is directly linked to the order of the convergence, we do not list the convergence rate directly.

Contents

1 Introduction

The one dimensional linear advection can be formulated as

$$\begin{aligned} u_t + a(x,t)u_x &= 0, \quad x \in I \subset \mathbb{R}, t > 0 \\ u(x,0) &= u_0(x), \quad x \in I \subset \mathbb{R} \end{aligned} \tag{1}$$

In practice, we can assume $I = \mathbb{R}$, or I is finite and periodic condition is imposed on u. Besides, the one dimensional Burgers equation can be stated as

$$\begin{aligned} u_t + uu_x &= 0, \quad x \in \mathbb{R}, t > 0 \\ u(x,0) &= u_0(x) \end{aligned} \tag{2}$$

which can be generalized to

$$\begin{aligned} u_t + f(u)_x &= 0, \quad x \in \mathbb{R}, t > 0 \\ u(x,0) &= u_0(x) \end{aligned} \tag{3}$$

2 Linear advection equation

2.1 Finite difference method

In this section, we adopt the notion in the textbook. And restate the results below. In the following, we assume $\nu = \frac{a_j^m \tau}{h}$.

Upwind scheme

$$U_j^{m+1} = U_j^m - \frac{\nu}{2}(U_{j+1}^m - U_{j-1}^m) + \frac{|\nu|}{2}(U_{j+1}^m + U_{j-1}^m - 2U_j^m) \tag{4}$$

The CFL condition is

$$|\nu| \leq 1 \tag{5}$$

and the order of convergence is $\mathcal{O}(\tau + h)$

Lax-Friedrichs scheme

$$U_j^{m+1} = \frac{1}{2}(U_{j+1}^m + U_{j-1}^m) - \frac{a_j^m \tau}{2}(U_{j+1}^m - U_{j-1}^m) \tag{6}$$

The CFL condition is

$$|\nu| \leq 1 \tag{7}$$

Under such condition, the scheme is locally $\mathbb{L}^2$ and $\mathbb{L}^\infty$ stable, and the ordere of convergence is $\mathcal{O}(\tau + h^2/\tau)$

Lax-Wendroff scheme

$$U_j^{m+1} = -\frac{1}{2}\nu(1-\nu)U_{j+1}^m + (1-\nu^2)U_j^m - \frac{1}{2}\nu(1+\nu)U_{j-1}^m \tag{8}$$

The CFL condition is

$$|\nu| \leq 1 \tag{9}$$

Beam-Warming scheme

$$U_j^{m+1} = \begin{cases} \frac{1}{2}(1-\nu)(2-\nu)U_j^m + \nu(2-\nu)U_{j-1}^m - \frac{1}{2}\nu(1-\nu)U_{j-2}^m, & \nu \geq 0 \\ \frac{1}{2}(1+\nu)(2+\nu)U_j^m - \nu(2+\nu)U_{j+1}^m + \frac{1}{2}\nu(1+\nu)U_{j+2}^m, & \nu \leq 0 \end{cases} \tag{10}$$

The CFL condition is

$$|\nu| \leq 2 \tag{11}$$

2.2 Boundary condition

Periodic boundary condition Assume I is a period of the initial function $u_0(x)$. Notice that $a(x,t)$ is also periodic in x for every t. Hence, we can use the periodicity to define the value outside I.

Finite interval boundary condition The values of u on $x = x_l,\ x = x_r$ have been stipulated. Hence, we need only consider inner grid points. However, the Beam-Warming scheme may involve value outside the boundary on the grid line $j = 1,\ n-1$. Hence, we utilize Lax-Wendroff scheme under such case.

Real line For $t = t_0, I = [x_{right}, x_{left}]$, we set up grids such that $t_0 = m\tau, x_{right} - x_{left} = nh$. Then, we determine the domain of dependence, and construct the initial layer, which contain $2m + n + 1$ points. Then, we iteratively move forward in the time direction until the m-th layer. On the j-th layer, there are $2(m-j) + n + 1$ grid points. Except the Beam-Warming scheme, no boundary condition needs to be imposed. However. for the Beam-Warming scheme, we still turn to Lax-Wendroff scheme when points outside the grid are involved.

3 Quasilinear equation

3.1 Finite difference method

In this setting, we consider more general cases:

$$\begin{aligned} u_t + (f(u))_x = 0, \quad x \in \mathbb{R}, t > 0 \\ u(x,0) = u_0(x) \end{aligned} \tag{12}$$

The CFL condition is

$$\max_{u\in\mathcal{U}} |f'(u)| \le \frac{h}{\tau} \tag{13}$$

where $\mathcal{U}$ is the solution regime. Besides, the numerical scheme must be of conservative form. We summarize the schemes below.

3.1.1 Upwind type scheme

Upwind scheme

$$\begin{aligned} U_j^{m+1} =& U_j^m - \frac{\tau}{2h}\{[(1+sgn(a^m_{j+\frac{1}{2}}))f(U_j^m) + (1-sgn(a^m_{j+\frac{1}{2}}))f(U^m_{j+1})] \\ &-[(1+sgn(a^m_{j-\frac{1}{2}}))f(U^m_{j-1}) + (1-sgn(a^m_{j-\frac{1}{2}}))f(U_j^m)] \end{aligned} \tag{14}$$

where

$$a^m_{j\pm\frac{1}{2}} = \begin{cases} \frac{f(U^m_{j\pm1})-f(U^m_j)}{U^m_{j\pm1}-U^m_j}, & U^m_{j\pm1} \neq U^m_j \\ 0, & U^m_{j\pm1} = U^m_j \end{cases} \tag{15}$$

Roe scheme

$$U_j^{m+1} = U_j^m - \frac{\tau}{2h}(f(U^m_{j+1}) - f(U^m_{j-1}) - |a_{j+\frac{1}{2}}|(U_{j+1}-U_j) + |a_{j-\frac{1}{2}}|(U_j - U_{j-1}))) \tag{16}$$

where

$$a^m_{j\pm\frac{1}{2}} = \begin{cases} \frac{f(U^m_{j\pm1})-f(U^m_j)}{U^m_{j\pm1}-U^m_j}, & U^m_{j\pm1} \neq U^m_j \\ 0, & U^m_{j\pm1} = U^m_j \end{cases} \tag{17}$$

Huang's scheme

$$\begin{aligned} U_j^{m+1} = U_j^m - \frac{\tau}{2h}(f(U^m_{j+1}) - f(U^m_{j-1}) \\ - sign(f'(\frac{U_j^m + U^m_{j+1}}{2}))(f(U^m_{j+1}) - f(U^m_j)) + sign(f'(\frac{U_j^m + U^m_{j-1}}{2}))(f(U^m_j) - f(U^m_{j-1}))) \end{aligned} \tag{18}$$

Engquist and Osher scheme

$$U_j^{m+1} = U_j^m - \frac{\tau}{2h}(f(U^m_{j+1}) - f(U^m_{j-1}) - \int_{U_j^m}^{U^m_{j+1}} |f'(u)|du + \int_{U^m_{j-1}}^{U^m_j} |f'(u)|du) \tag{19}$$

We adopt Simpson integration method to approximate the integral here.

3.1.2 Second-order scheme

MacCormack's scheme

$$\begin{cases} \hat{U}_j^n = U_j - \frac{\tau}{h}(f(U_{j+1}^m) - f(U_j^m)) \\ U_j^{m+1} = \frac{1}{2}(U_j^m + \hat{U}_j^m) - \frac{\tau}{2h}(f(\hat{U}_j^m) - f(\hat{U}_{j-1}^m)) \end{cases} \tag{20}$$

The following two are modifications of the Lax-Wendroff scheme.

Richtmyer scheme

$$\begin{cases} U_{j+\frac{1}{2}}^{m+\frac{1}{2}} = \frac{1}{2}(U_j^m + U_{j+1}^m) - \frac{\tau}{2h}(f(U_{j+1}^m) - f(U_j^m)) \\ U_j^{m+1} = U_j^m - \frac{\tau}{h}(f(U_{j+\frac{1}{2}}^{m+\frac{1}{2}}) - f(U_{j-\frac{1}{2}}^{m+\frac{1}{2}})) \end{cases} \tag{21}$$

Lax-Wendroff scheme

$$\begin{aligned} U_j^{m+1} =& U_j^m - \frac{\tau}{2h}(f(U_{j+1}^m) - f(U_{j-1}^m)) \\ &+ \frac{\tau^2}{2h^2}[(a_{j+\frac{1}{2}}^m(f(U_{j+1}^m) - f(U_j^m)) - a_{j-\frac{1}{2}}^m(f(U_j^m) - f(U_{j-1}^m))] \end{aligned} \tag{22}$$

where $a_{j\pm\frac{1}{2}}^m = f'(\frac{1}{2}(U_j^m + U_{j\pm1}^m))$.

3.2 Initial and boundary condition

We can assume the interval we are to consider is (x_{left}, x_{right}). And the grid point is $x_j = (j - \frac{1}{2})h + x_{left}$, $h = \frac{x_{right} - x_{left}}{n}, j = 0, 1, \ldots, n+1$. The initial condition can be formulated as

$$U_j^0 = \frac{1}{h}\int_{x_{j-\frac{1}{2}}}^{x_{j+\frac{1}{2}}} u_0(x)\mathrm{d}x, \quad j = 1, 2, \ldots, n \tag{23}$$

In our setting, there are no boundary conditions imposed. In order to strengthen our analysis, we consider the following setting:

$$\begin{aligned} u_t + f(u)_x = 0, &\quad x \in (0,1), t > 0 \\ u(x,0) = u_0(x), &\quad x \in (0,1) \\ u(0,t) = u^0(t), &\quad t \geq 0 \\ u(1,t) = u^1(t), &\quad t \geq 0 \end{aligned} \tag{24}$$

Define

$$F_{1/2}^{m+1/2} = \frac{1}{\tau}\int_{t_m}^{t_{m+1}} f(u^0(t))dt \tag{25}$$

and use the upwind scheme.
Besides, for the Richtmyer scheme, $F_{j+1/2}^{m+1/2} = f(U_{j+1/2}^{m+1/2}$. Since $U_{1/2}^{m+1/2}$ and $U_{n+1/2}^{m+1/2}$ can be

explicitly calculated, thus, minor modification needs to be done to fit the situation. For the sake of simplicity, we only implement these two schemes to represent the first order and second order scheme. To get a explicit solution, we suppose

$$u(x,t) = \sqrt{\frac{x}{1+t}} \tag{26}$$

hence,

$$u_t + u^2 u_x = 0 \tag{27}$$

4 Results

The numerical results are generated by main.m, which takes "condition" as input to specify different cases.

4.1 Linear case

4.1.1 Finite interval

We manufacture a function defined on $[0,1] \times \mathbb{R}^2$ as follows

$$u(x,t) = \exp(x-t),\ (x,t) \in [0,1] \times \mathbb{R}^2 u_0(x) = \exp(x),\ x \in [0,1] \tag{28}$$

We calculate the value at $t = 1$. Choose a scheme, and execute

```
err_linear_finite(scheme_choice)
```

Error figures are plotted in the figure 1, 2, 3, 4.

4.1.2 Discontinuous aperiodic initialization

The initial function and grid parameters are identical to Example 2.1 in the reference. Set $n = 100, 400$ separately, and execute

```
main('linear-discontinous-infinite')
```

We can get the result in the figure 5 6 in the appendix. (case1_1.fig, case1_2.fig in the folder)

4.1.3 Continuous aperiodic initialization

The initial function and grid parameters are identical to Exercise 2.1 in the reference. Execute

```
main('linear-continous-infinite')
```

We can get the result in the figure 7 8 9 in the appendix. (case2_1.fig, case2_2.fig, case2_3.fig for $t = 2, 4, 8$ in the folder)

4.1.4 Discontinuous periodic initialization

The initial function and grid parameters are identical to Exercise 2.1 in the reference. Execute

```
main('linear-discontinous-infinite')
```

We can get the result in the figure 10 in the appendix. (case3.fig in the folder)

4.1.5 Continuous periodic initialization

We set

$$u_0(x) = sin(\pi x) \tag{29}$$

The region we consider is $[-1, 1] \times \{t = t_0\}$, and $h = \frac{1}{250}, dt = 0.0032$. We consider $t_0 = 4$ and $t_0 = 16$. Execute

```
main('linear-continous-periodic')
```

The results, figure 11 12, are plotted in the appendix. (case4_1.fig, case4_2.fig in the folder) In this specific case, after setting $x \in [-1, 1], \nu = 0.8$, we execute

```
convergence_test('linear')
```

and get the l^∞ error listed in the section 5.1. It is clear that the convergence error of the upwind and Lax-Friedrichs schemes are of the first order, and the Lax-Wendroff and Beam-Warming schemes are of the second order.

4.1.6 Summary

The experiments validate that high-order accurate schemes gives superior performance for equal resolution, but the second-order accurate scheme suffers from the numerical oscillations while the first-order accurate scheme tends to smooth the discontinuities. The oscillations move behind of the discontinuities for the Lax-Wendroff scheme and ahead of the discontinuities for the Beam-Warming scheme. When the mesh is refined, the oscillations do not decrease in magnitude but increase in frequency, but all the numerical results tend to the real solutions. The decay of amplitude of the first-order scheme can be observed in Figure 11 and 12, and the phase error of the second-order scheme can be observed in Figure 8 and 9. In the mean time, Figure 8 and 9 illustrate that first order scheme cannot capture the high-frequency parts well.

4.2 Quasilinear case

We focus on the Burgers' equation, and assume the initial value is periodically defined on the real line. Similar to previous work, we still determine the domain of dependence first and then move forward in time.

4.2.1 Riemann problem

We will consider two cases: rarefaction and shock.

Rarefaction

$$u_0(x) = \begin{cases} 1, & x < 0 \\ 2, & x > 0 \end{cases} \tag{30}$$

Real solution:

$$u_0(x) = \begin{cases} 1, & x < t \\ x/t, & t \leq x \leq 2t \\ 2, & x \geq 2t \end{cases} \tag{31}$$

Shock

$$u_0(x) = \begin{cases} 2, & x < 0 \\ 1, & x > 0 \end{cases} \tag{32}$$

Real solution:

$$u_0(x) = \begin{cases} 2, & x < st \\ 1, & x > st \end{cases} \tag{33}$$

where $s = f(2) - f(1)$.
We consider the region $t = 0.5$ and $x \in [-2, 2]$. Then we execute the following code

```
main_burgers('Riemann');
```

We can get the result in the figure 13 in the appendix. (case5.fig in the folder).

4.2.2 Continuous problem

After specifying parameters in the main_burgers.m, execute

```
main_burgers('continuous');
```

We assume the initial data

$$u_0(x) = 0.5 + \sin(x) \tag{34}$$

We consider $t = 0.8$, as in figure 14 There is a transonic compression wave in the solution at $t = 0.8$ in the interval $[2.8, 4.2]$ before the shock is formed. If we set $t = 1.2$, we can clearly observe the shock in figure 16. Additionally, we set $t = 0.9$ in figure 15. (case6_1.fig case6_2.fig, case6_3.fig for $t = 0.8, 0.9, 1.2$ in the folder).
Obviously, the upwind type schemes, though of the first-order, outperforms the second-order schemes around the shock point.
When $t = 0.8, 0.9$, we will investigate the convergence rate. It is worth noticing that the real solution u at point (x, t) satisfy

$$u = 0.5 + sin(x - ut) \tag{35}$$

Hence, we can adopt Newton's method to iteratively solve the equation, the stopping criterion is that the error is less than 1e-6. Results are summerized in the section 5.2. We perform more detailed analysis when $t = 0.8, 0.84$. To visualize the results, execute

```
err_burgers_infinite(scheme_choice)
```

I plot the results in Figure 17 - 23, and store the figures in the folder case7_1.fig - case7_7.fig. The difference of the first-order and second-order method can be clearly recognized from different slopes of the l^∞ norm. We also plot l^2 norm besides as comparison.

4.2.3 Finite interval problem

Second order scheme For scheme_choice = 'Richtmyer middle' or 'Richtmyer Thompson', we execute

```
err_nonlinear_finite(scheme_choice)
```

and got the error plot in Figure 24 25. The l^∞ norm of error on the interval [0,1] is only $\mathcal{O}(h^{1/2})$, which is not satisfactory. By observing the error on [0,1], we discover that the error concentrate on the boundary. Hence, the most part of the error is induced by boundary conditions. If we restrict our attention on the interval [0.1,0.9], we will discover that the convergence of l^∞ norm satisfy our theoretical prediction. Order of convergence matches the order of the scheme.

First order scheme We use Thompson integration to estimate the integral 25. Since $f' > 0$, we use the first order extrapolation on the right side of the boundary. We execute

```
err_nonlinear_finite('upwind')
```

and got the error plot in Figure 26. The l^∞ norm of error on the interval [0,1] is only $\mathcal{O}(h^{1/2})$, and on the interval [0.1, 0.9] is $\mathcal{O}(h)$, which satisfies our theoretical prediction.

5 Appendix A: Table collections

5.1 Linear case

Table 1: Upwind Scheme

n \ t	0.8	1.6	2.4	3.2	4
100	0.031089	0.061211	0.090398	0.118677	0.146076
200	0.015667	0.031089	0.046269	0.061212	0.07592
300	0.010472	0.020835	0.031089	0.041236	0.053714
400	0.007865	0.015667	0.023409	0.031089	0.038709
500	0.006297	0.012554	0.018771	0.02495	0.031089

Table 2: Lax-Friedrichs Scheme

n \ t	0.8	1.6	2.4	3.2	4
100	0.068562	0.13242	0.191908	0.247322	0.29894
200	0.034903	0.068587	0.101095	0.132469	0.162748
300	0.023407	0.046267	0.068591	0.090393	0.112557
400	0.017608	0.034906	0.051899	0.068593	0.084993
500	0.014111	0.028024	0.04174	0.055262	0.068594

Table 3: Lax-Wendroff Scheme

n \ t	0.8	1.6	2.4	3.2	4
100	0.00119	0.00238	0.00357	0.00476	0.00595
200	0.000298	0.000595	0.000893	0.00119	0.001488
300	0.000132	0.000265	0.000397	0.000529	0.017415
400	7.44E-05	0.000149	0.000223	0.000298	0.000372
500	4.76E-05	9.52E-05	0.000143	0.00019	0.000238

Table 4: Beam-Warming Scheme

n \ t	0.8	1.6	2.4	3.2	4
100	0.000794	0.001587	0.002381	0.003174	0.003968
200	0.000198	0.000397	0.000595	0.000794	0.000992
300	8.82E-05	0.000176	0.000265	0.000353	0.016314
400	4.96E-05	9.92E-05	0.000149	0.000198	0.000248
500	3.18E-05	6.35E-05	9.53E-05	0.000127	0.000159

5.2 Quasilinear case

5.2.1 Upwind type

Table 5: Upwind scheme

	100	200	300	400	500
0.8	0.186162	0.107104	0.074861	0.057888	0.04723
0.9	0.293026	0.229091	0.169763	0.139003	0.117408

Table 6: Roe scheme

	100	200	300	400	500
0.8	0.186162	0.107104	0.074861	0.057888	0.04723
0.9	0.293026	0.229091	0.169763	0.139003	0.117408

Table 7: Huang scheme

	100	200	300	400	500
0.8	0.186162	0.107104	0.074861	0.057888	0.04723
0.9	0.293026	0.229091	0.169763	0.139003	0.117408

Table 8: Engquist & Osher scheme

	100	200	300	400	500
0.8	0.18524	0.107104	0.074861	0.057888	0.04723
0.9	0.29259	0.229091	0.169763	0.139003	0.117408

5.2.2 Second-order scheme

Table 9: Richtmyer scheme

	100	200	300	400	500
0.8	0.022397	0.006392	0.002923	0.00166	0.001067
0.9	0.077019	0.031238	0.016419	0.00996	0.006629

Table 10: Lax-Wendroff scheme

	100	200	300	400	500
0.8	0.028229	0.008144	0.00372	0.002115	0.001376
0.9	0.091247	0.037793	0.020216	0.012406	0.008316

Table 11: MacCormack scheme

	100	200	300	400	500
0.8	0.027718	0.007981	0.003641	0.002101	0.001362
0.9	0.089928	0.037323	0.019998	0.012285	0.00824

6 Appendix B: Figure collections

In Figure 1 - Figure 4, the upper part is the error on $t = 1$ under different n, where $m = 2n$. And the lower left part represent the l^∞-norm, the lower right part represent the l^2-norm.

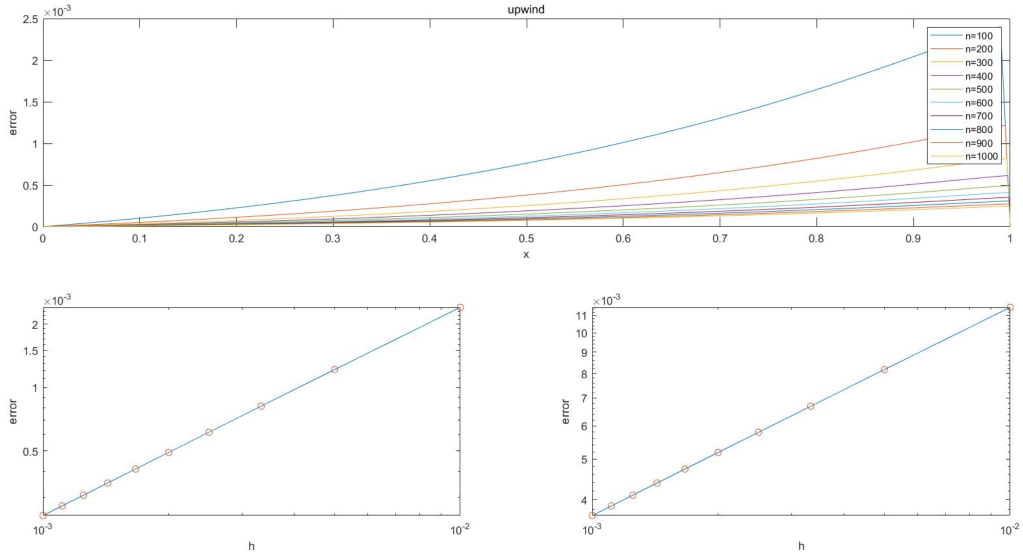

Figure 1: Finite initialization, upwind scheme, order 1

In Figure 17 - Figure 23, the upper part is the error on $t = 0.8/0.9$ under different n, where $m = 2n$. And the lower left part represent the l^∞-norm, the lower right part represent the l^2-norm.

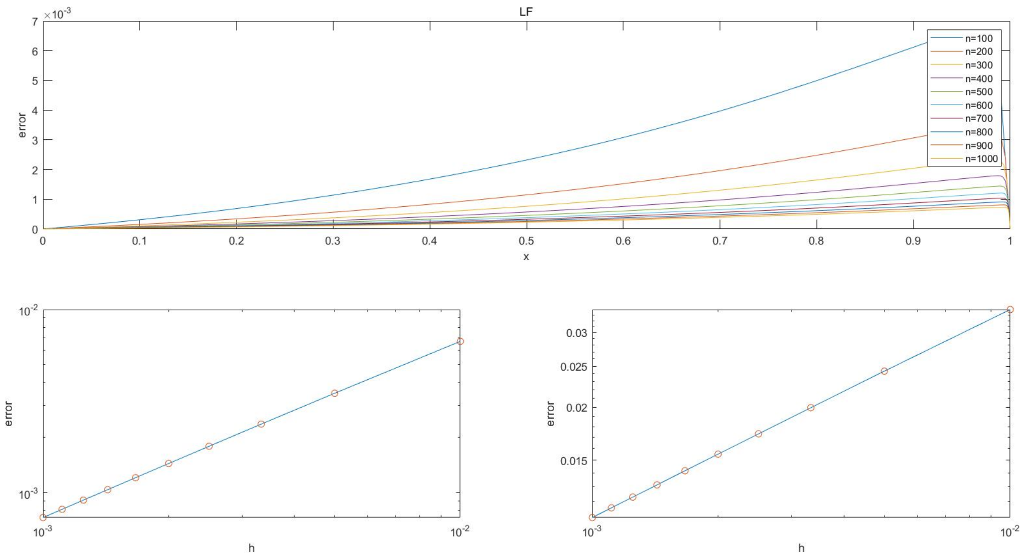

Figure 2: Finite initialization, LF scheme, order 1

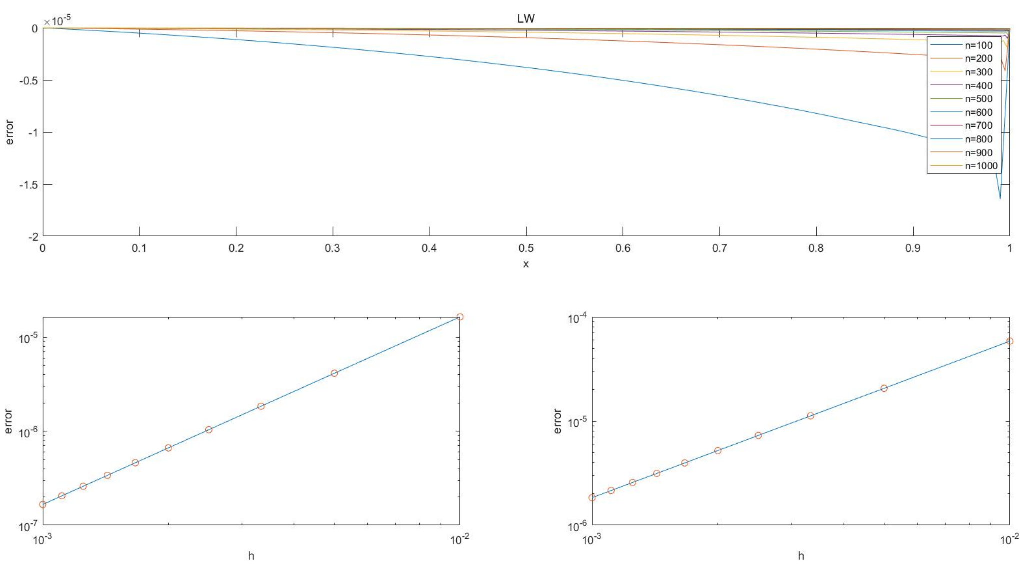

Figure 3: Finite initialization, LW sheme, order 2

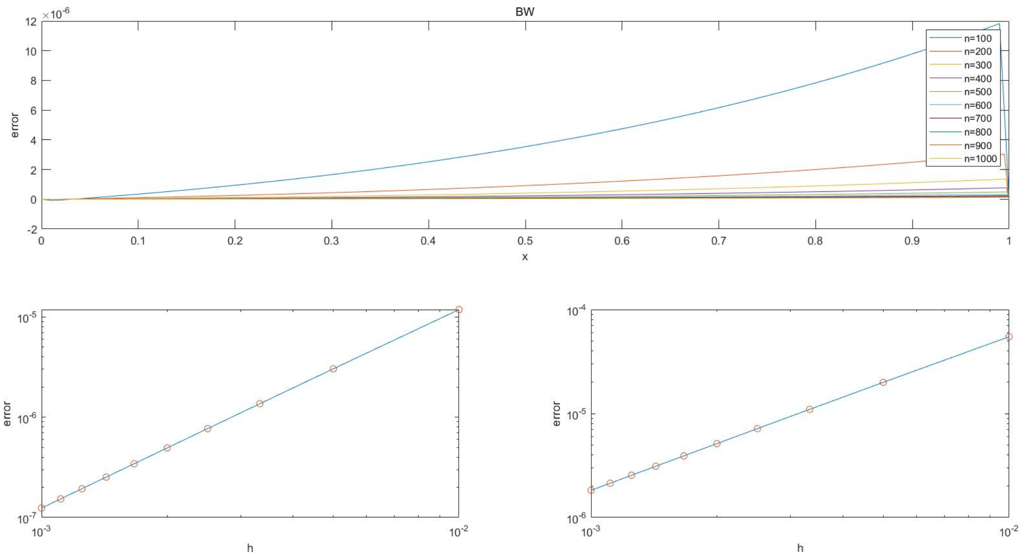

Figure 4: Finite initialization, BW scheme, order 2

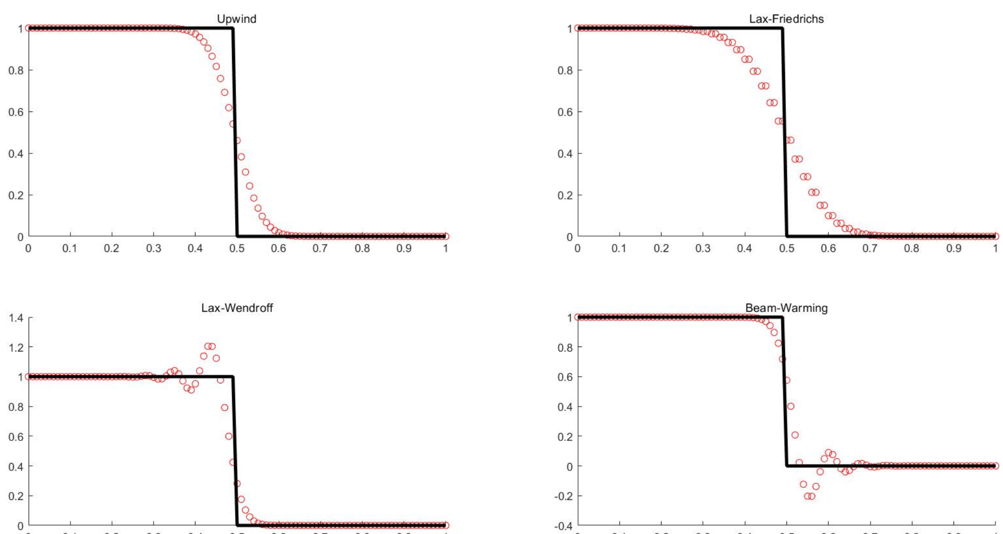

Figure 5: Discontinuous aperiodic initialization, $h = 0.01$

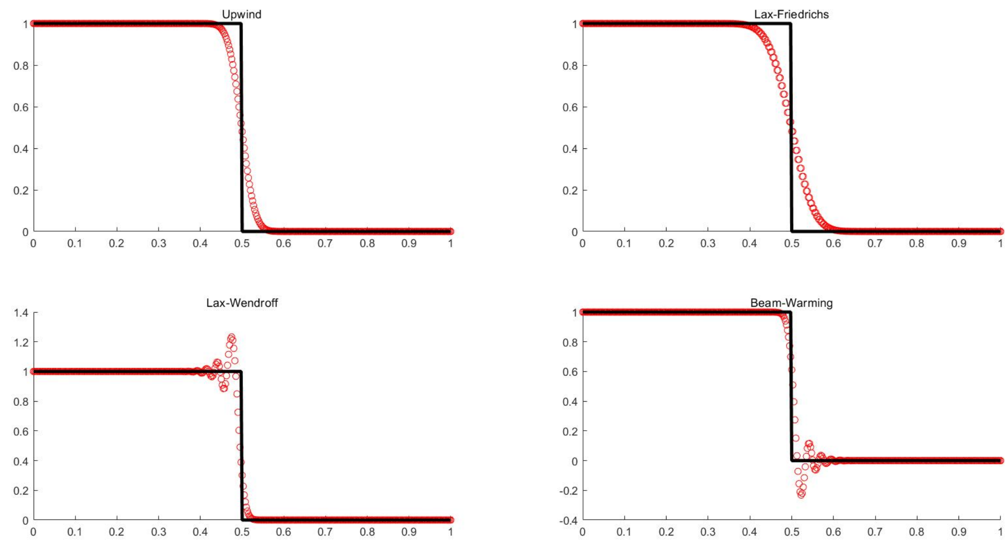

Figure 6: Discontinuous aperiodic initialization, $h = 0.0025$

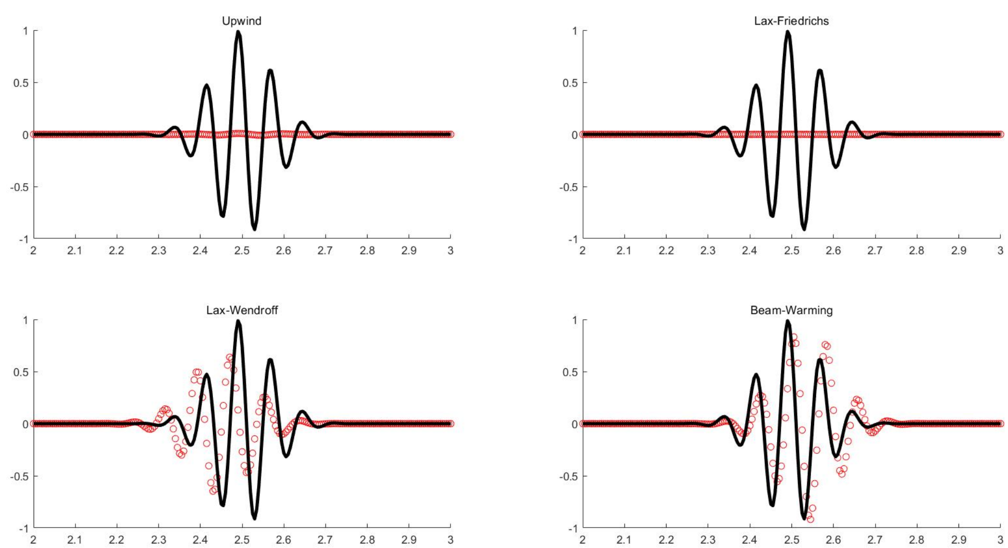

Figure 7: Continuous aperiodic initialization, $t = 2$

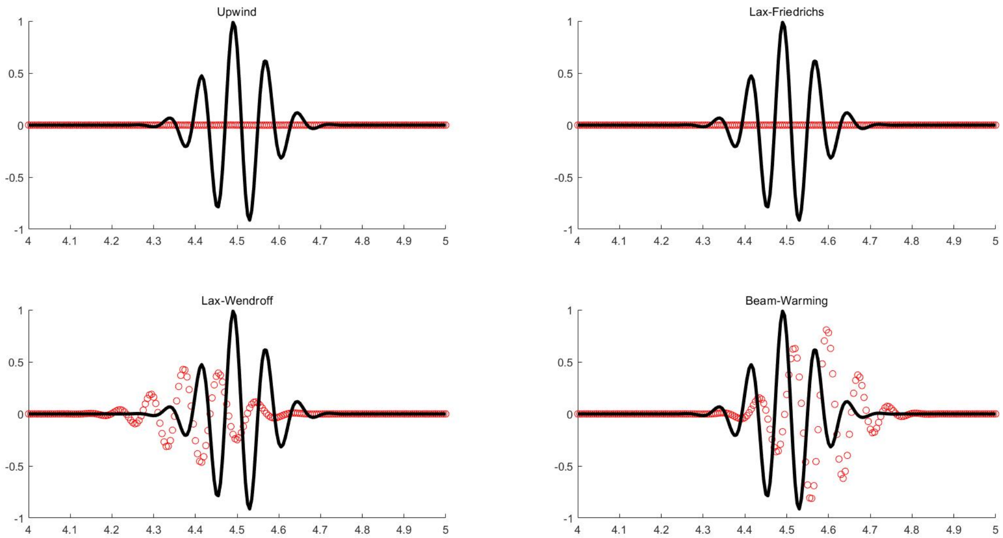

Figure 8: Continuous aperiodic initialization, $t = 4$

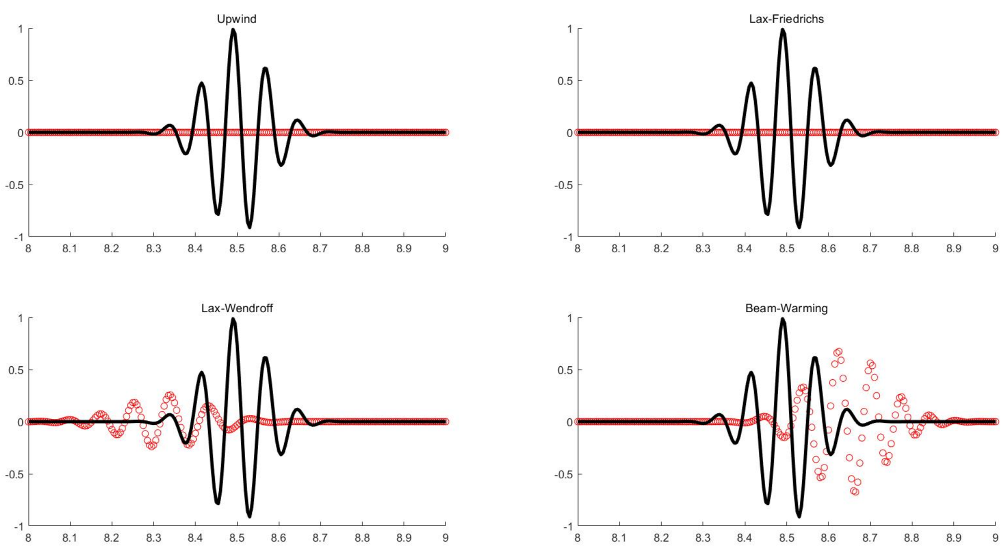

Figure 9: Continuous aperiodic initialization, $t = 8$

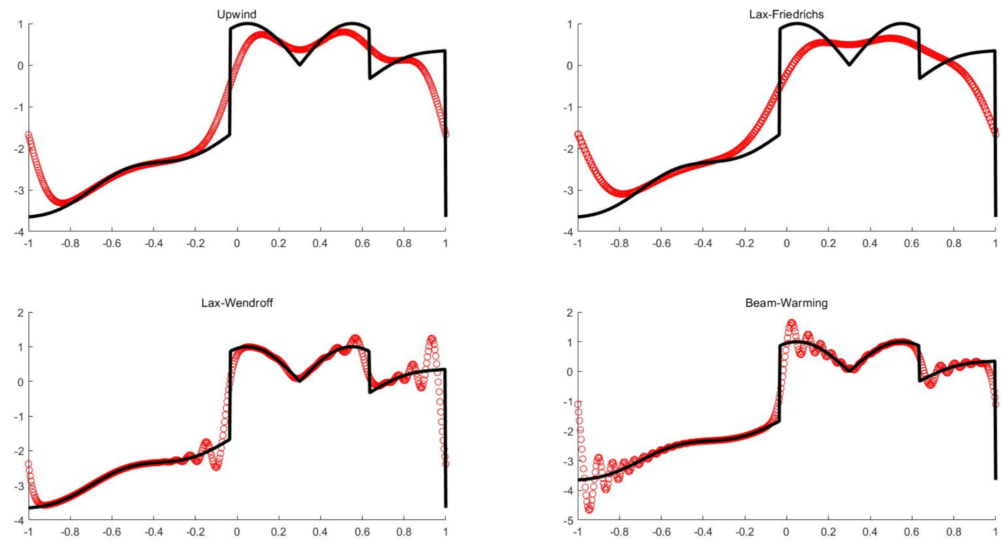

Figure 10: Discontinuous periodic initialization

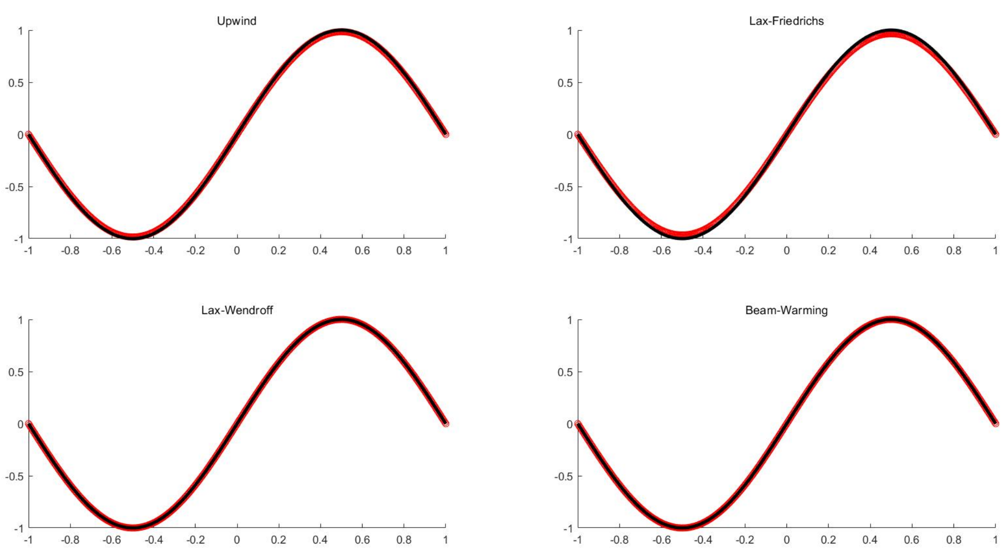

Figure 11: Continuous periodic initialization, $t_0 = 4$

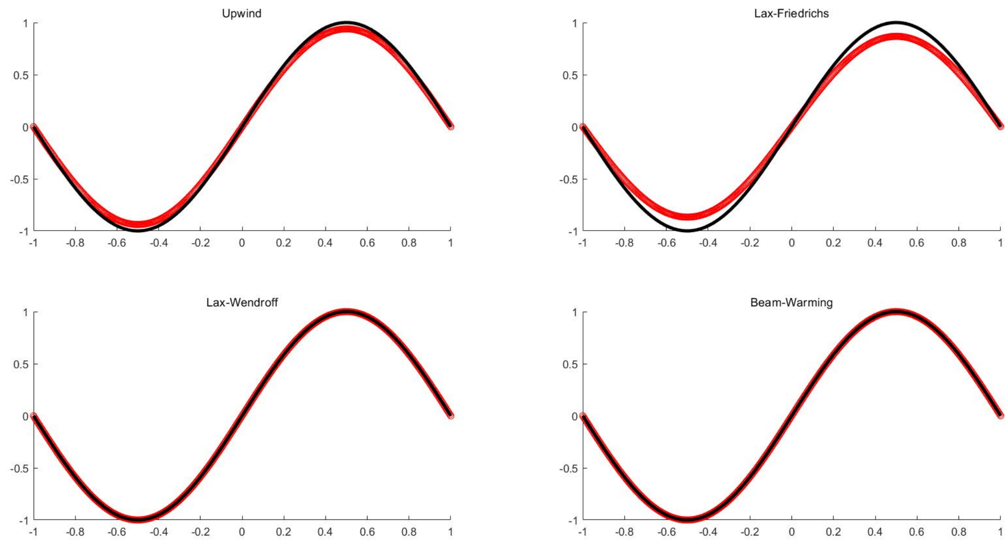

Figure 12: Continuous periodic initialization, $t_0 = 16$

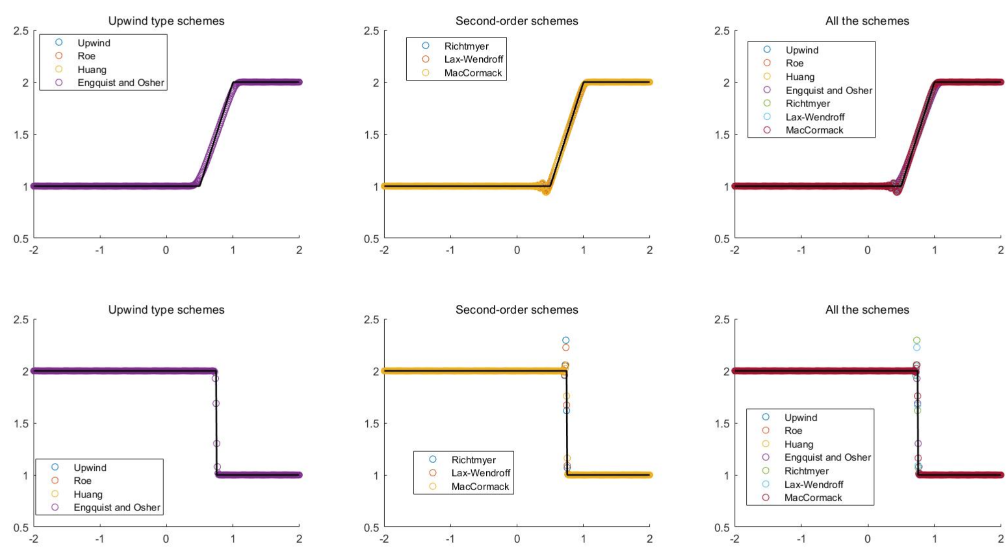

Figure 13: Riemann problem, $t = 0.5$. The first row: rarefaction wave; the second row: shock wave.

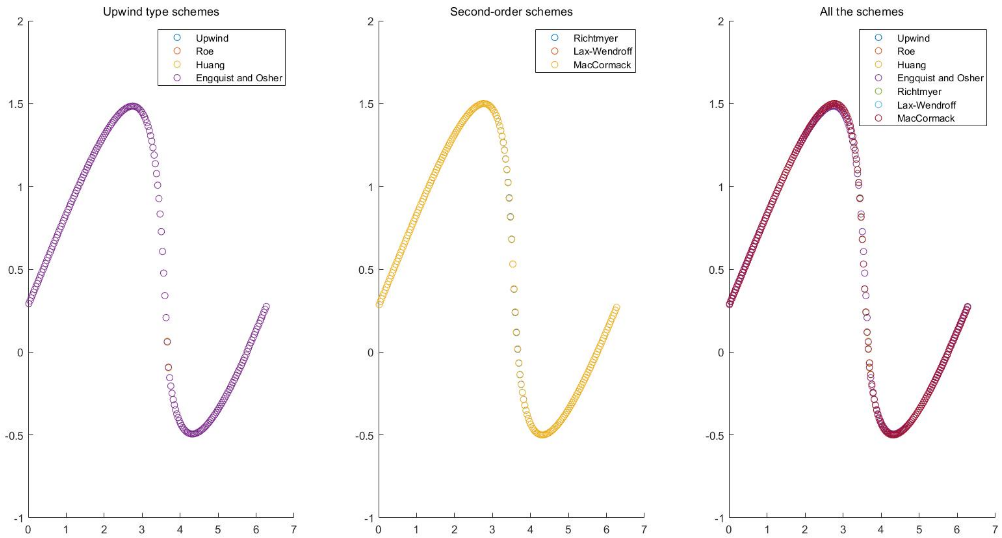

Figure 14: Continuous problem, $t = 0.8$

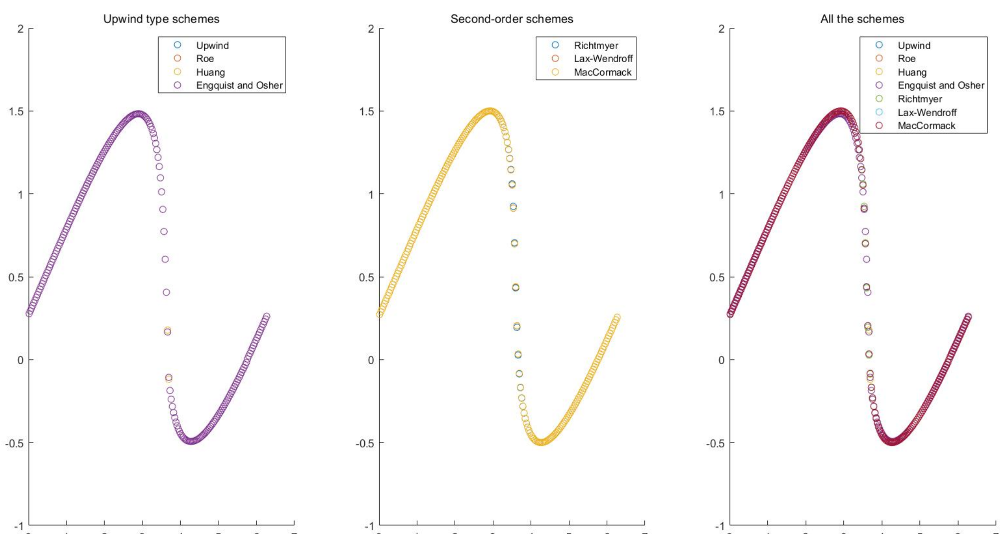

Figure 15: Continuous problem, $t = 0.9$

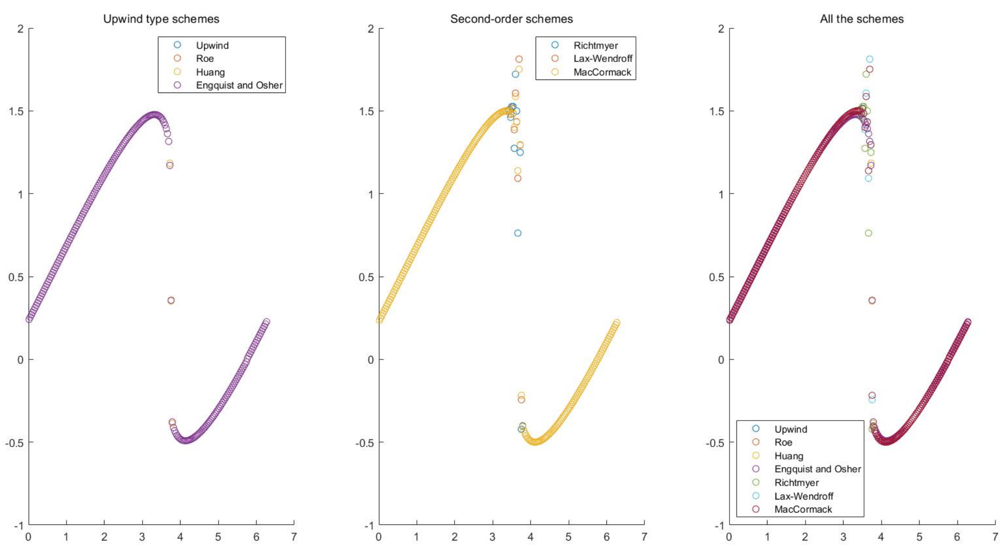

Figure 16: Continuous problem, $t = 1.2$, shock occurs

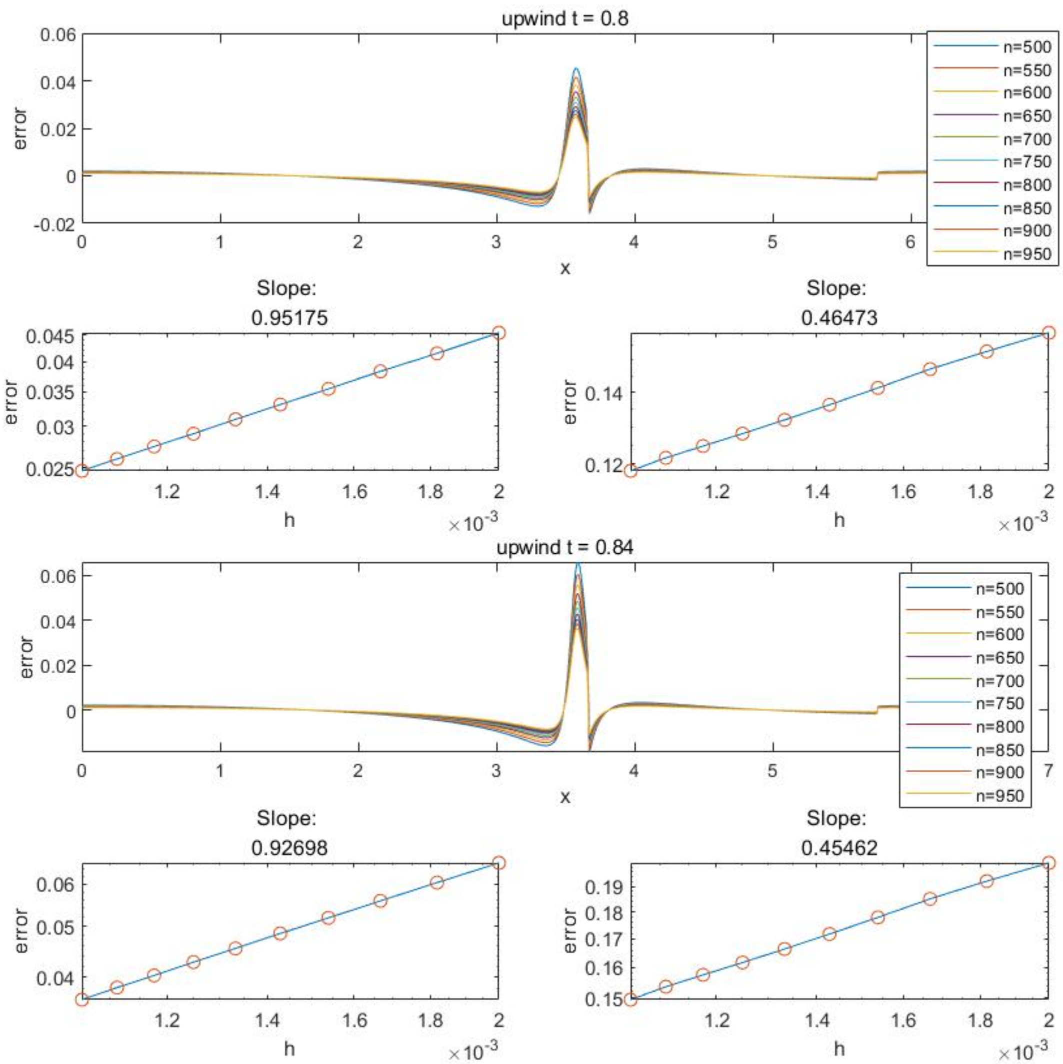

Figure 17: Burgers equation, upwind scheme

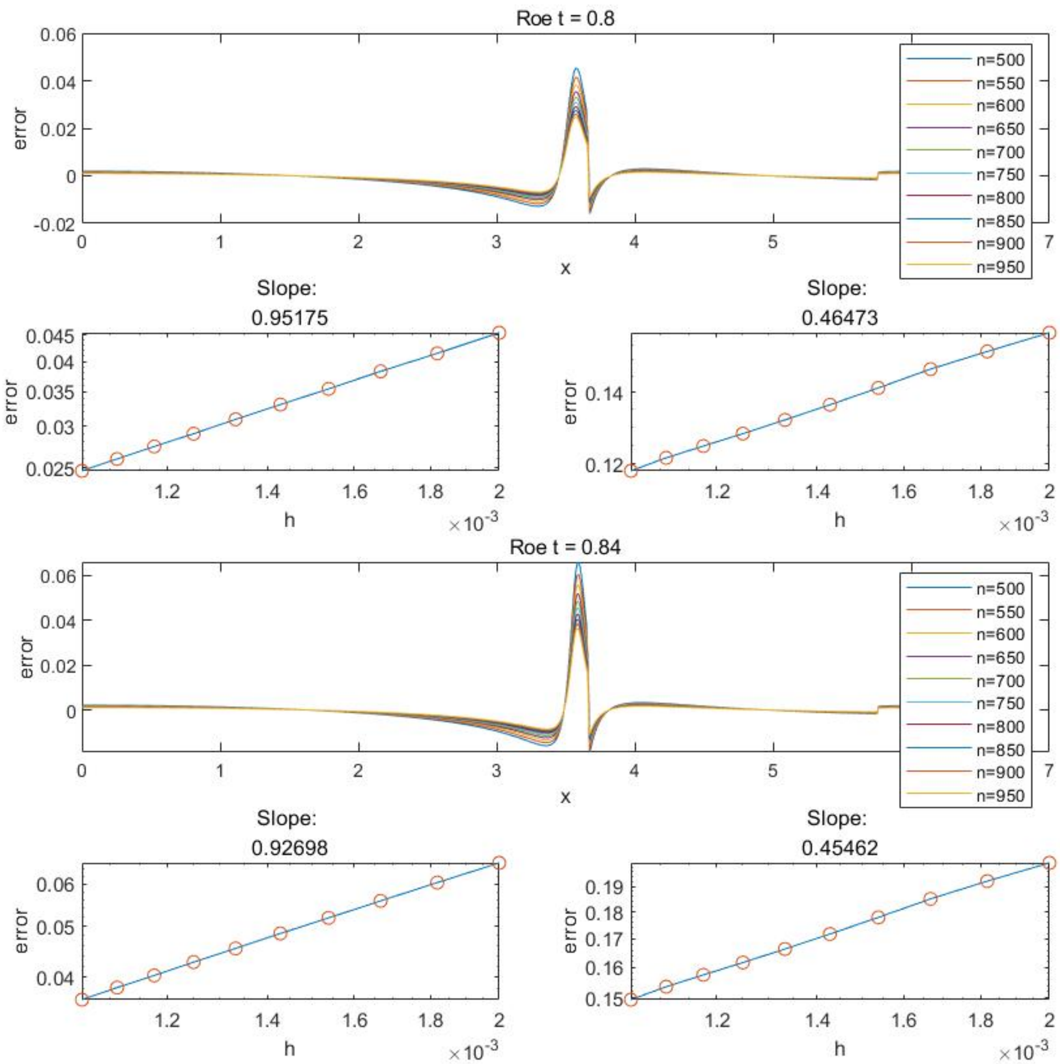

Figure 18: Burgers equation, Roe scheme

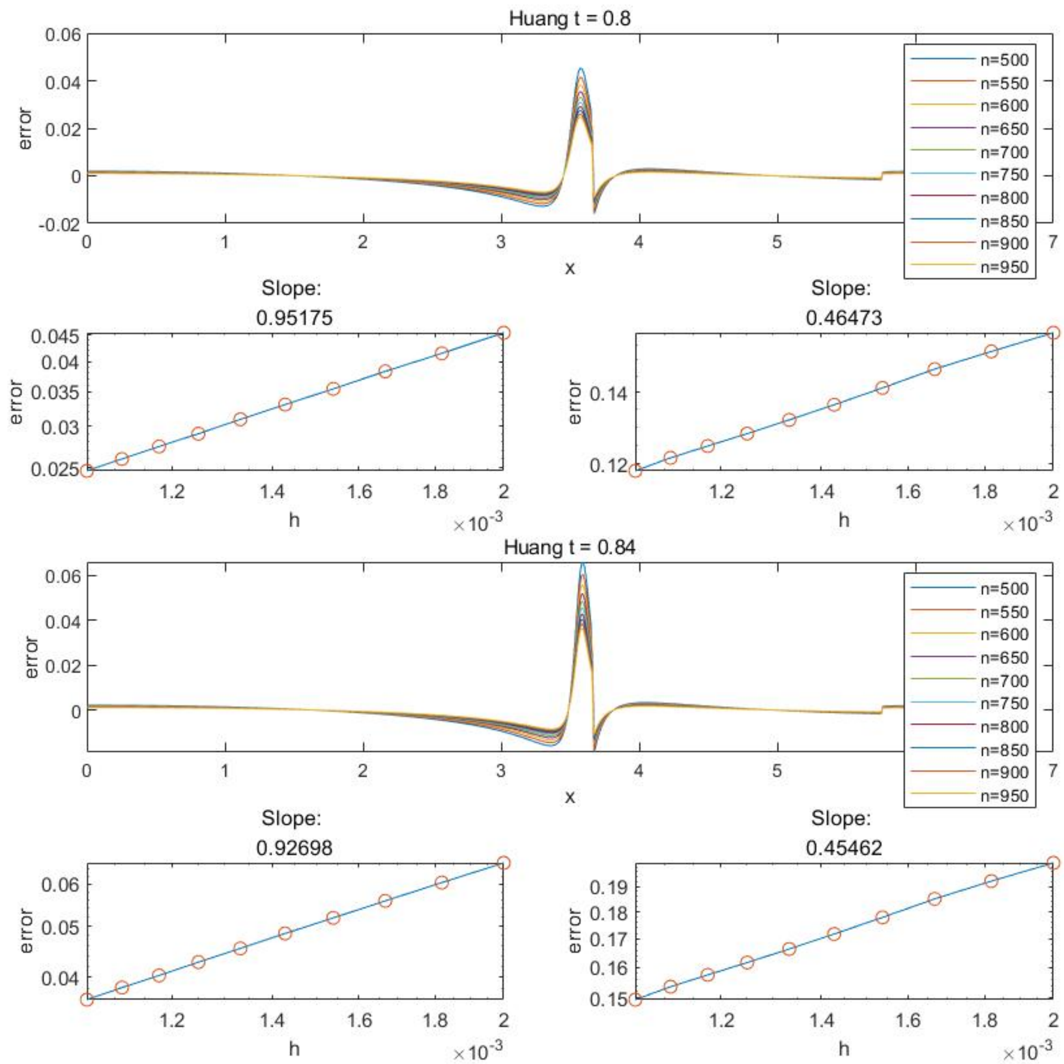

Figure 19: Burgers equation, Huang scheme

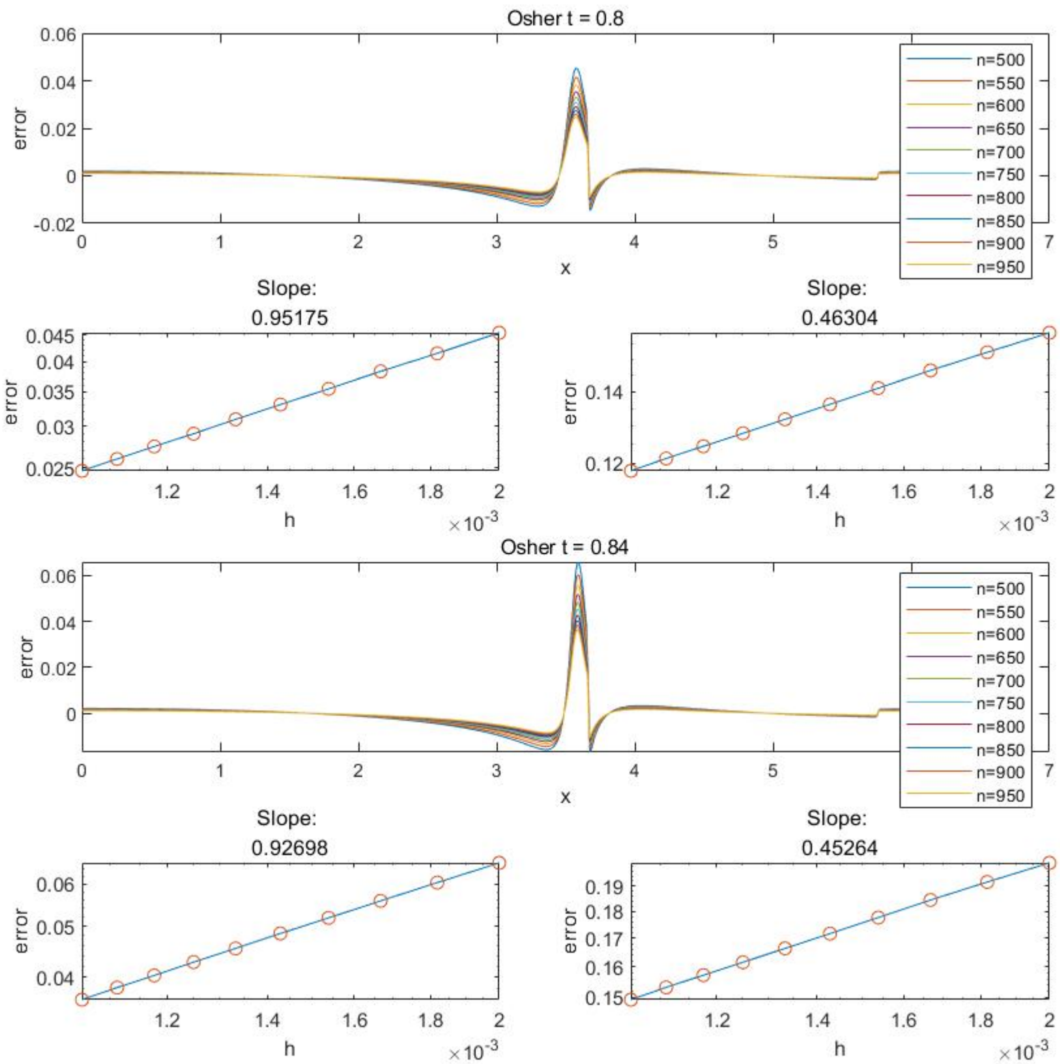

Figure 20: Burgers equation, Osher scheme

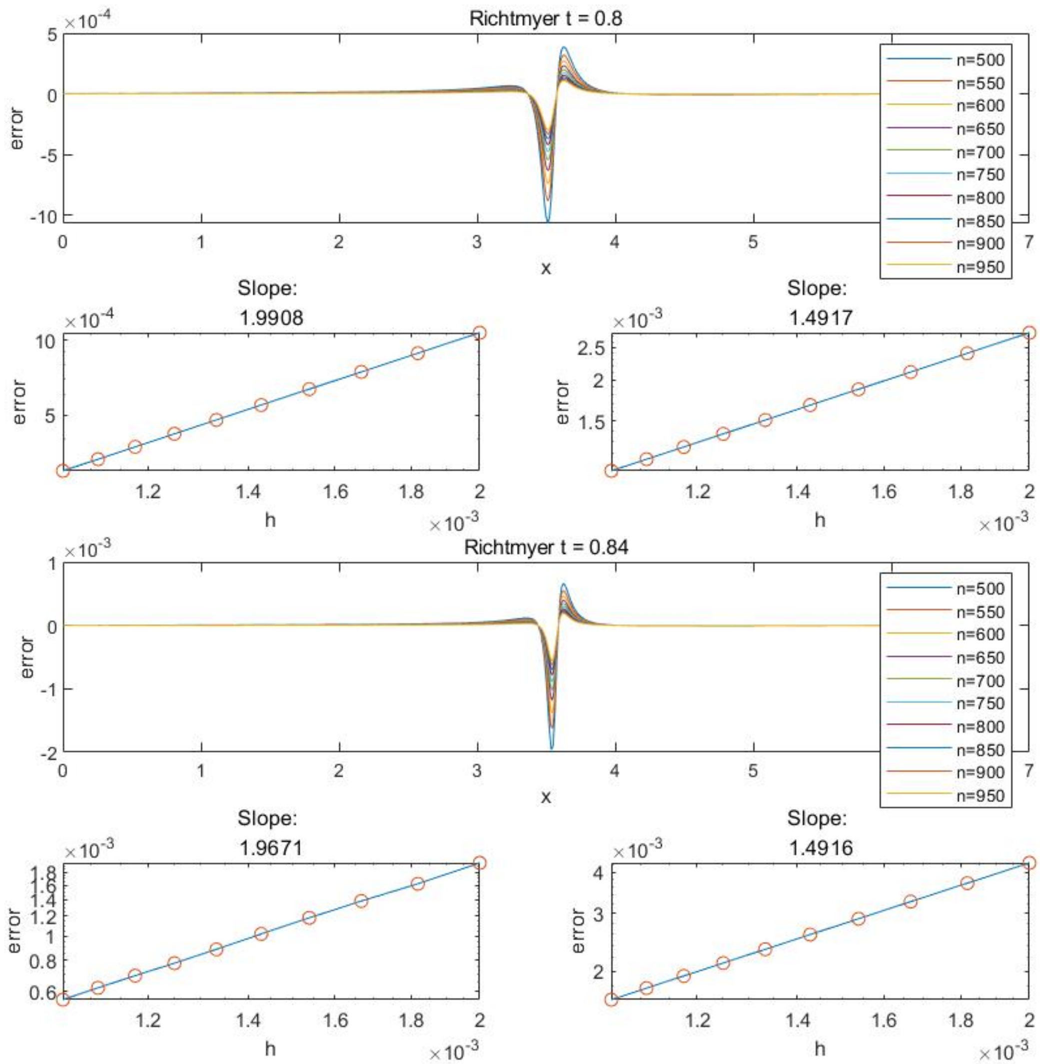

Figure 21: Burgers equation, Richtmyer scheme

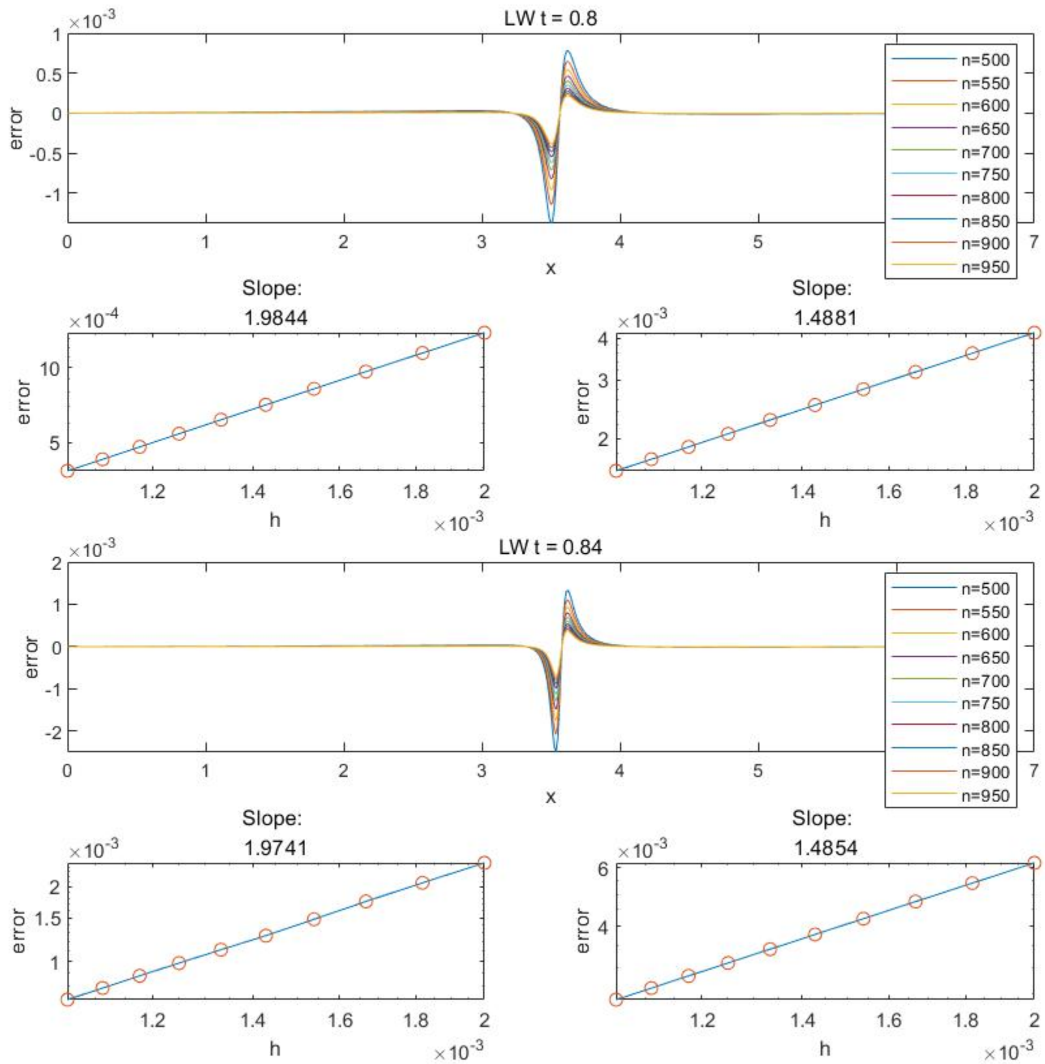

Figure 22: Burgers equation, LW scheme

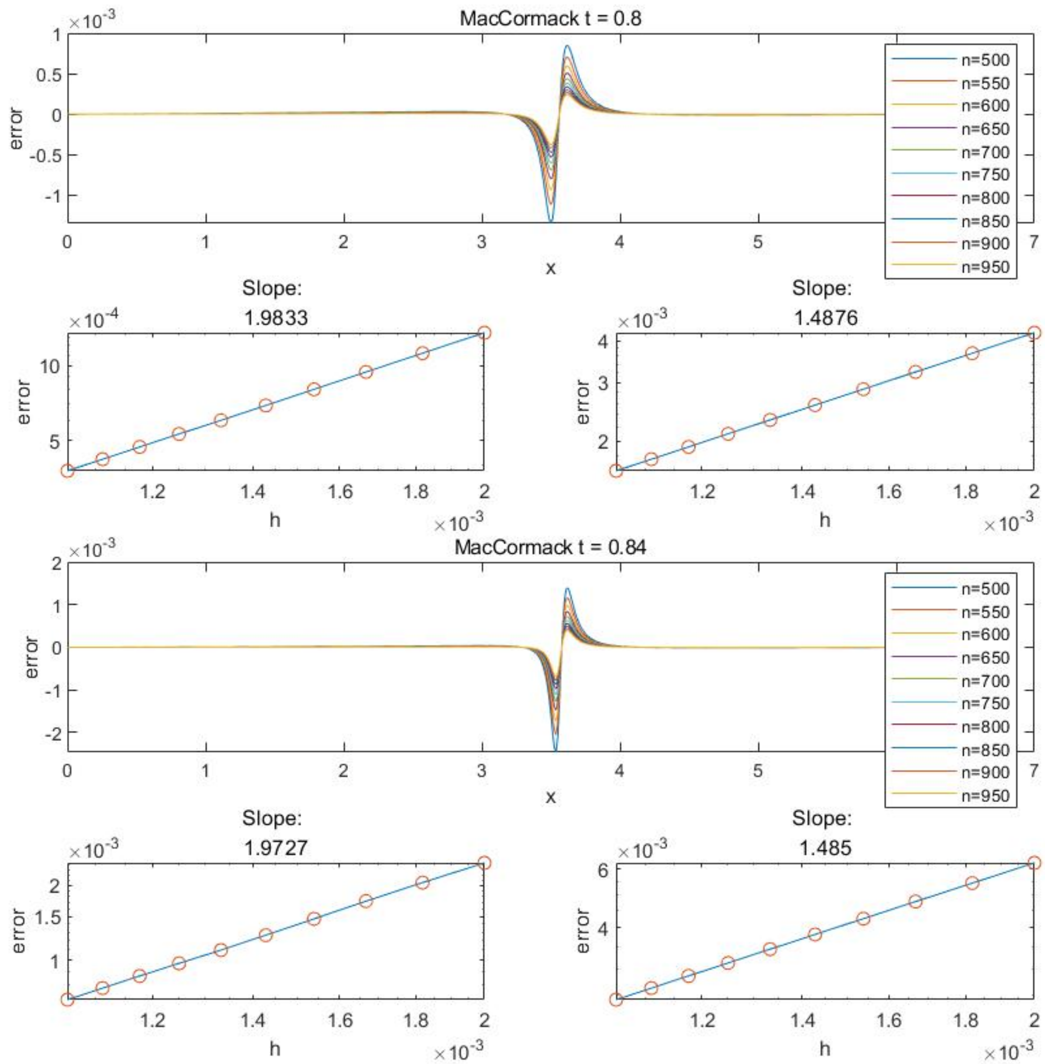

Figure 23: Burgers equation, MacCormack scheme

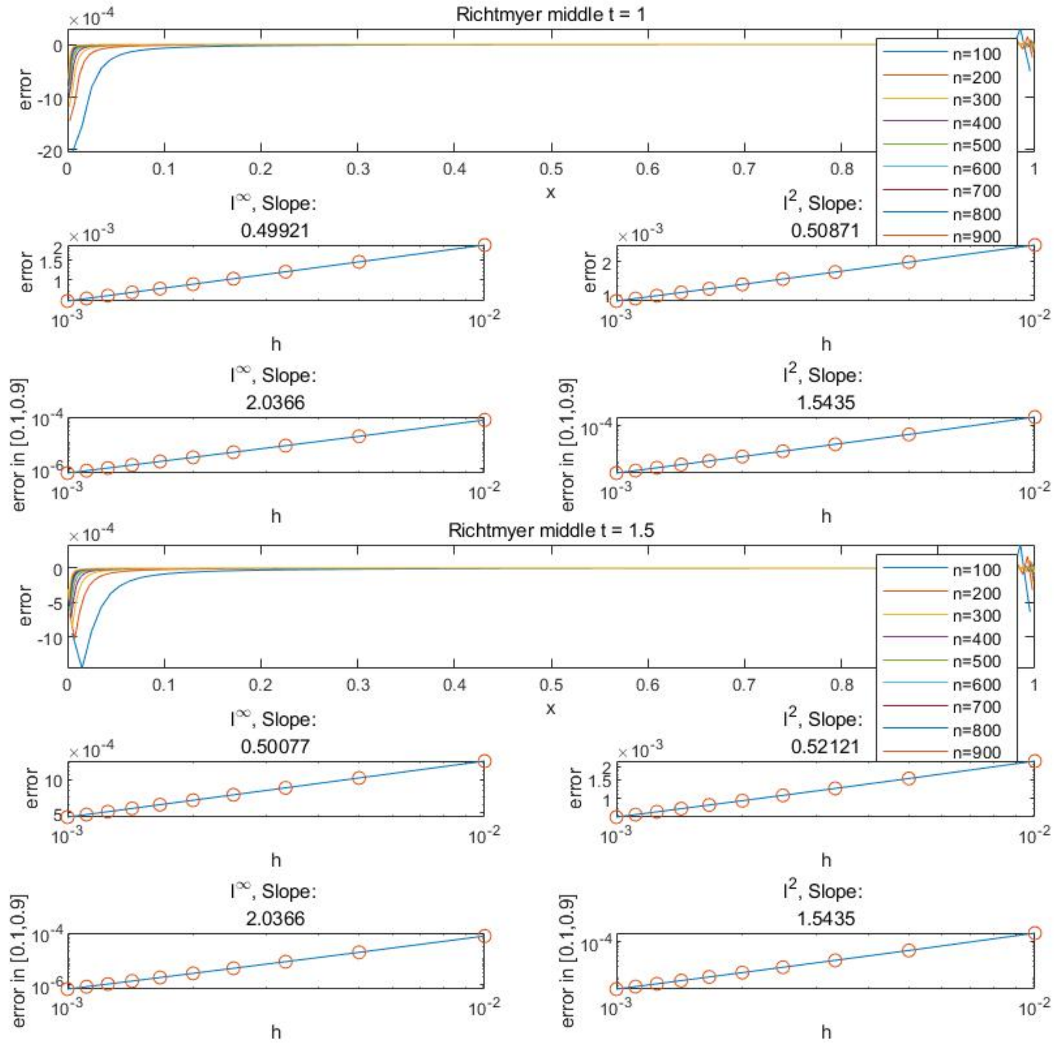

Figure 24: Boundary condition, Richtmyer scheme, middle point integration

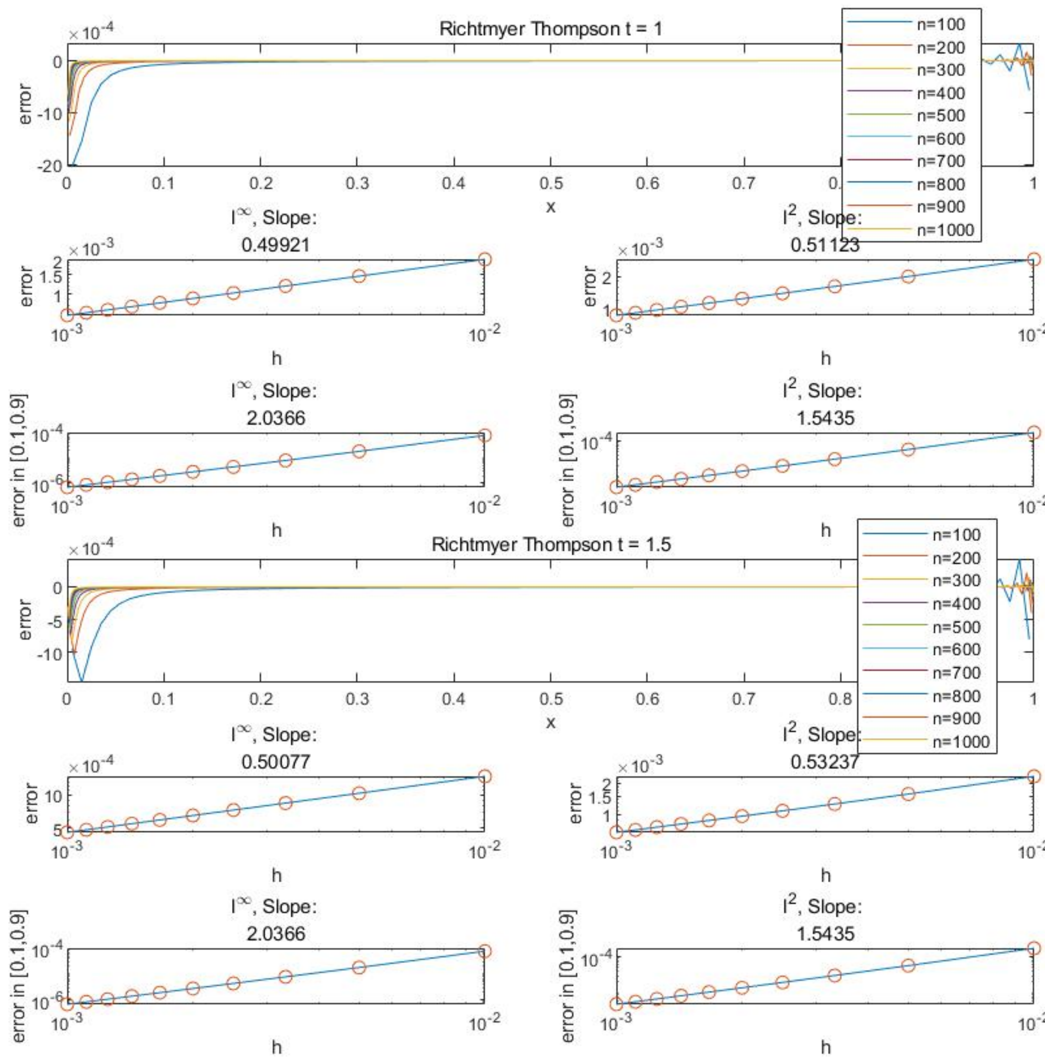

Figure 25: Boundary condition, Richtmyer scheme, Thompson integration

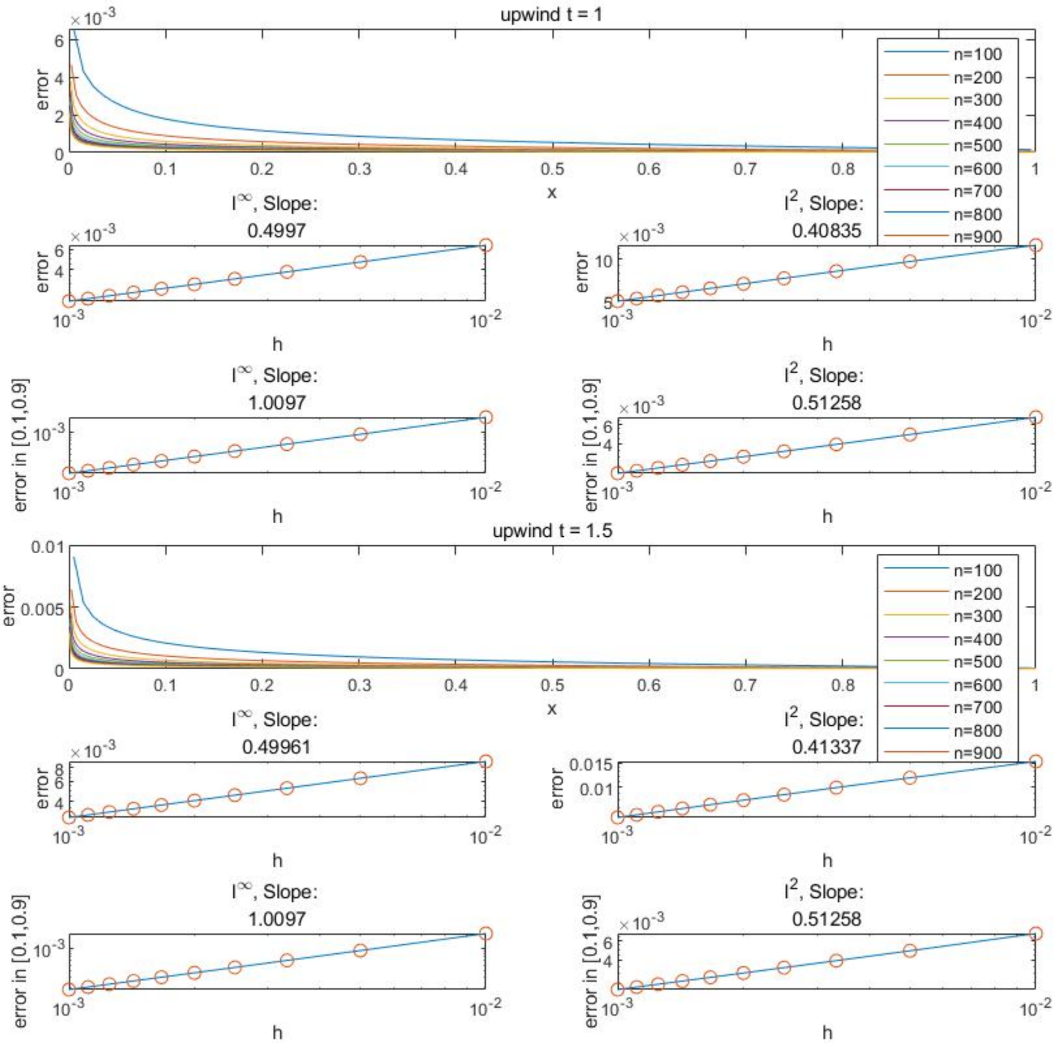

Figure 26: Boundary condition, Upwind scheme

7 Appendix C: Codes explanations

1. Before executing any scripts, execute

   ```
   addpath(genpath(pwd))
   ```

   in all the folders.

2. The folder "function" contains the different initial values and boundary values, the folder "Figure collection" collects all the figure in the ".fig" format to identify the details of the figures. Moreover, the main folder contain the main scripts that we will illustrate below.

3. linear_periodic_solver.m deals with periodic initial value, linear_infinite_solver.m discards the conditions that the initial value is periodic, nonlinear_solver.m solves the quasilinear equation, linear_finite_solver.m solves the linear equation on a finite interval, nonlinear_boundary_solver.m solves the quasilinear equation on a finite interval.

4. The exact steps to generate the figures and tables are included in the main content.

5.